MOLECULAR PHARMACOLOGY, 24:521-531

Pharmacophor Requirements of the Aldose Reductase Inhibitor Site

PETER F. KADOR AND NORMAN E. SHARPLESS

Laboratory of Vision Research, National Eye Institute, and Laboratory of Chemical Physics, National Institute of Arthritis, Diabetes, and Digestive and Kidney Diseases, National Institutes of Health, Bethesda, Maryland 20205

Received August 26, 1982; Accepted July 6, 1983

SUMMARY

Recent experimental results suggesting that diabetic pathology can at least in part be directly controlled through inhibition of the enzyme aldose reductase (alditol:NADPH oxidoreductase, EC 1.1.1.21) have spurred great interest in the development of specific inhibitors of this enzyme. Specific structural and electronic similarities of apparently diverse aldose reductase inhibitors have been observed through basic studies which utilize computer molecular modeling, molecular orbital calculations, known structure-activity relationships, and protein-modification reagents such as 2-bromo-4′-nitroacetophenone. From these similarities, a model of the aldose reductase inhibitor site has been postulated along with the pharmacophor requirements for the inhibitors—guidelines which should aid in the rational design of new inhibitors.

INTRODUCTION

Aldose reductase (alditol:NADPH oxidoreductase, EC 1.1.1.21) is an enzyme in the sorbitol pathway which utilizes the coenzyme NADPH to reduce hexose sugars to their respective sugar alcohols. This enzyme has been shown to initiate cataract formation through the reduction of excess glucose to sorbitol. The intracellular accumulation of sorbitol produces a hyperosmotic effect which results in cellular swelling and subsequent cataract formation (1). Evidence is also mounting that aldose reductase may be involved in other diabetic complications such as corneal wound healing defects, neuropathy, retinopathy, nephropathy, and platelet aggregation (1–3).

Although currently no treatment for these diabetic complications exists, inhibition of this enzyme represents a potentially direct pharmacological approach toward the treatment of these complications—an approach distinct from the improved control of blood sugar levels. Studies in diabetic animals indicate that the use of potent aldose reductase inhibitors can prevent cataract formation (4) and a decreased rate of corneal re-epithelialization (1, 5). Moreover, in pilot clinical trials the administration of aldose reductase inhibitor resulted in improved motor nerve conduction velocity (neuropathy) in diabetic patients (6). These results, which indicate that diabetic pathology can at least in part be directly controlled by drug therapy, have spurred great interest in the development of specific aldose reductase inhibitors.

In the search for potent inhibitors, many compounds of diverse structure have been identified. Kinetic studies indicate that these compounds appear to interact with the enzyme at a site independent of either the substrate or nucleotide cofactor fold. The inhibitory activity of compounds containing the benzopyran ring system has been correlated with their ability to undergo a charge-transfer interaction at a reactive carbonyl in position 4 (7). Moreover, studies with enantiomers of 1,3-dioxo-1*H*-benz[de]isoquinoline-2(3*H*)-2′-propionic acid, chiral analogues of Alrestatin, *1*, and enantiomers of the sterically constrained spirohydantoin Sorbinil, *3*, suggest that aldose reductase can differentiate stereochemically between inhibitors (8).

Differences in the susceptibility of aldose reductase from various sources to inhibition have also been reported (9, 10). Moreover, these studies, which suggest that currently no "universally potent" inhibitor exists, indicate the need for potent new inhibitors. Here we propose a general model for the inhibitor site and present the minimal structural requirements for an aldose reductase inhibitor. These results should serve as a guideline in the rational design of more potent and selective aldose reductase inhibitors.

EXPERIMENTAL PROCEDURES

Inhibitor assay. RLAR[1] and HPAR were prepared as previously described (7, 8). Enzyme activity was spectrophotometrically assayed at 340 nm in a Gilford 2400-2 automated spectrophotometer using 10 mM DL-glyceraldehyde as substrate (7). Inhibitor IC_{50} values were obtained from simple linear regressions of the Marquardt-Levenberg iterative curve-fitting algorithm of the National Institutes of Health MLAB computer program as previously described (8).

Alkylation studies. HPAR purified by affinity chromatography (11)

[1] The abbreviations used are: RLAR, rat lens aldose reductase; HLAR, human lens aldose reductase; HPAR, human placental aldose reductase; BLAR, bovine lens aldose reductase; BrNAP, 2-bromo-4′-nitroacetophenone; CNDO, complete neglect of differential overlap; GEMO, geometrie moleculaire (geometry and energy of organic molecules); LEMO, lowest empty molecular orbitals; CPK, Cory-Pauling-Koltun.

0026-895X/83/060521-11$02.00/0

was dialyzed against 0.1 M Na,K-phosphate buffer (pH 7.2) and then incubated with either 1 mM BrNAP (Aldrich Chemical Company, recrystallized from tetrahydrofuran-hexane) or 1 mM 4-nitrobenzenesulfonyl fluoride (Pierce) dissolved in 5% dimethyl sulfoxide. Following a specified time interval of 15 min to overnight, the enzyme solution was dialyzed through a PD-10 column prepacked with Sephadex G-25M (Pharmacia Fine Chemicals) and then spectrophotometrically assayed. Kinetic analyses were conducted using the BINKIN2 procedure of the National Institutes of Health PROPHET computer system as previously described (8).

Computer modeling. Molecular models of the inhibitors were generated on the National Institutes of Health PROPHET computer system (12), using the make molecule command. Three-dimensional structures of these molecules were then constructed using the compute model command. This program generates a molecular conformation according to either standard or specific bond lengths, bond angles, and torsion angles and information contained in its ring dictionary. Coordinates for the hydantoin ring were obtained from crystal coordinates (13); coordinates for all other heterocyclic ring systems were calculated from the available GEMO energy minimizer program run on the National Institutes of Health DEC-10. This program utilizes classical nonquantum mechanical relationships to estimate the preferred, minimal conformational energy structure of a molecule (14). After energy minimization, the orientation of the molecule could be altered using the ORMOL procedure, and additional selective conformational changes could be introduced through simple turn molecule and twist bond commands. Molecular electronic charge distribution and energy calculations were estimated by using a quantum mechanical CNDO/2 program which utilized the atomic coordinates of the inhibitors (15).

The molecular coordinates for the inhibitors were also introduced onto the National Institutes of Health DEC-10 X-ray program, and the molecular models were superimposed onto each other in real-time using the Evans and Sutherland system (16). Similarly, the tyrosine and arginine amino acids were introduced to the superimposed inhibitor model and the 3-dimensional CPK models generated. A molecular model of the inhibitor site was then generated on PROPHET from the coordinates of the superimposed inhibitor A-ring and the two amino acids. Inhibitors could be readily superimposed onto the model, and the intermolecular distances between the inhibitor and its binding site could be estimated within 0.10 Å. Intramolecular distances could be determined from vector analysis, and the distance of an atom from a least-squares plane passing through a specified set of atoms could be estimated with a root mean square error of less than 0.011.

Inhibitors. 3,4-Dihydroxyfluorenone, *8*, was a gift of Dr. D. W. Baston (17), and 2-(4′-hydroxyphenyl-6-carboxy-4*H*-chromen, *32*, was prepared as previously described (18). IC_{50} values of Compounds *1*, *3*, and *11–22* assayed against BLAR were estimated as described above from published data (19–21). The IC_{50} values for Compounds *24* and *28–30*, assayed against RLAR, and the xanthone, *7*, assayed against RLAR, were similarly estimated (22, 23). With the exception of 1-phenyl-spiro-indole-1,2,3*H*-2-oxo-3,4′-imidazolidine-2,5-dione, *10* (24), all other biological data have been previously reported (8–11, 25).

RESULTS AND DISCUSSION

A wide variety of compounds can inhibit aldose reductase, ranging from long-chain fatty acids to ring systems containing either the pyranone skeleton or its modifications or analogues. These include (among others) flavones, chromones, thiochromones, quinolones, xanthones, fluorenones, coumarins, and chalcones (7–10, 19–24, 26). Table 1 shows a variety of these inhibitors, including the well-known Alrestatin (1,3-dioxo-1*H*-benz[de]isoquinoline-2(3*H*)acetic acid), *1*; 7-hydroxy-4-oxo-4*H*-chromen-2-carboxylic acid, *2*; Sorbinil (*S*-6-fluoro-spirochroman-4,4′-imidazolidin-2′,5′-dione), *3*; and quercetin (2-(3,4-dihydroxy-phenyl)-3,5,7-trihydroxy-4-

TABLE 1

Examples of aldose reductase inhibitors

LEMO values were calculated from planar molecular conformations necessary to fit the inhibitor site (Figs. 3–5).

Compound	no.	IC_{50} RLAR μM	CNDO/2 LEMO	Compound	no.	IC_{50} RLAR μM	CNDO/2 LEMO
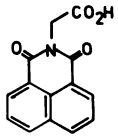	1	1.5	.0095	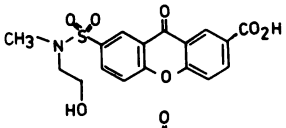	6	0.01*	.0447
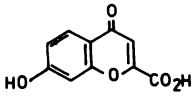	2	2.2	.0417	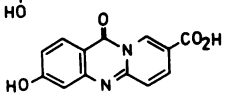	7	1.3	.0524
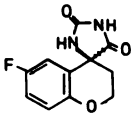	3	0.07	.0983	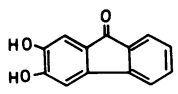	8	1.7	.0220
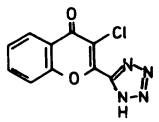	4	2.5	.0185	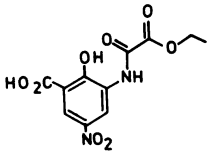	9	0.2	.0614
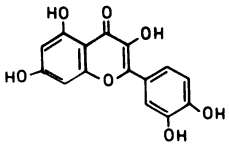	5	0.8	.0510	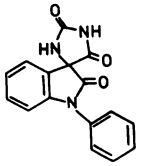	10	NA	.1098

*rabbit lens AR

oxo-4*H*-chromen), *5*. Kinetically, all of these inhibitors, with the exception of the spiro-indole, *10*, display either noncompetitive or uncompetitive inhibition, indicating that these compounds do not compete with either the substrate or nucleotide cofactor site (7, 8, 21, 22). Moreover, competition studies suggest that all of these inhibitors interact reversibly at a common site on the aldose reductase enzyme (inhibitor site). Although the specific biological properties of the spiro-indole, *10*, have not been reported (24), examination of other hydantoins indicate that they also possess similar kinetics (5). Since drug-protein interactions are dependent upon both steric and electronic parameters, the ability of these compounds to inhibit aldose reductase should be related to certain electronic and structural similarities.

Various electronic properties associated with a molecule can be estimated through molecular orbital calculations. From these calculations, an important quantum chemical index governing molecular charge-transfer interactions is the LEMO. From data obtained from simple Hückel molecular orbital calculations of flavonoids and chromones in which a correlation between inhibitory activity and LEMO was observed, it has been proposed that these aldose reductase inhibitors can undergo a charge-transfer interaction at a reactive carbonyl group by accepting a pair of electrons from the enzyme (7). Chaney *et al.* (27), using more sophisticated *ab initio* Hartree-Fock self-consistent field calculations with the molecular-fragments technique, proposed a similar charge-transfer mechanism for the ability of oxanilic, quinaldic, and benzopyran-2-carboxylic acids to act as antiallergy compounds. Many of these compounds also inhibit aldose reductase (26). A similar conclusion was also reached by Ferrell and co-workers (28) with CNDO/2 calculations of flavonoids and related compounds as potential phosphodiesterase inhibitors. Although comparisons between calculated molecular parameters are generally limited to analogues with similar ring systems or fragments, a comparison of the LEMOs calculated for compounds of Table 1 in a conformation suitable to fit the proposed inhibitor site versus their inhibitory activity against RLAR also suggests a similar relationship between the ability of these compounds to undergo a charge-transfer interaction and their ability to inhibit aldose reductase (Fig. 1). Moreover, an examination of the net charge distribution of aldose reductase inhibitors, illustrated in Table 2, reveals that a common feature of all of these compounds is the presence of polarized carbonyl groups capable of undergoing nucleophilic attack. For such an attack, however, an appropriate nucleophile is required. Its presence has been detected through the use of protein-modification reagents.

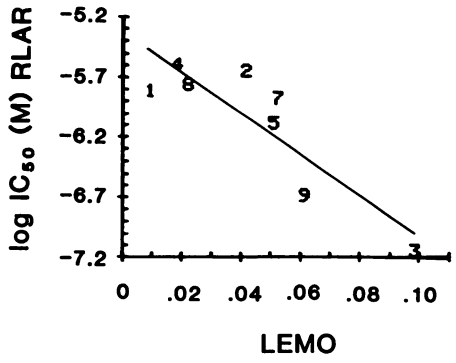

FIG. 1. *Comparison of the values of LEMO calculated for compounds in Table 1 versus their IC_{50} values obtained against RLAR*

Numbers correspond to the compound numbers in Table 1 (r = 0.087).

Addition of 1 mM BrNAP to purified HPAR results in the irreversible partial inhibition of this enzyme. Kinetic studies indicate this inhibition to be uncompetitive in nature with respect to the substrate (Fig. 2), whereas competition studies indicate that further inhibition of the alkylated enzyme cannot be readily accomplished with either 7-hydroxy-4-oxo-4*H*-chromen-2-carboxylic acid (IC_{50} 2 μM) or Sorbinil (IC_{50} 1 μM). Altering the concentration of NADPH also does not affect the inhibitory activity of BrNAP, indicating that BrNAP competes with known inhibitors for a site on the enzyme independent of either the substrate site or nucleotide cofactor fold. Through amino acid analysis of the acid hydrolysate of the alkylated enzyme, it was suggested that tyrosine may be the nucleophile and that reaction of HPAR with the tyrosine-specific modification-reagent 4-nitrobenzenesulfonyl fluoride (29) results in kinetically similar inhibition of the enzyme. Therefore, these results indicate that a nucleophilic amino acid, possibly tyrosine, exists at the specific inhibitor site.

Structural similarities among the apparently structurally diverse compounds in Table 1 can also be observed. All of these and other known related inhibitors possess either some fixed, planar molecular component or freely rotating aromatic substituents which can assume a planar conformation. In Table 1, Compounds *1–3* and *6–9* contain a planar aromatic component, and Compounds *4–5* and *10* contain both a planar ring and freely rotating aromatic substituent. Calculations of the 2-tetrazolyl-3-chloro-4-oxo-4*H*-chromen, *4*, indicates that in the preferred conformation the 2-tetrazyl group is nearly coplanar, approximately 12° out of the plane of the chromone ring, whereas in quercetin the 2-phenyl ring is approximately 89° out of plane. However, both compounds can assume coplanar conformations with the expenditure of 5.6 and 13.7 Kcal/mole, respectively. With the spirohydantoin *10*, the *N*-phenyl substituent was calculated to be coplanar with the indole ring. Although sterically constrained, the spirohydantoin *3* can assume three possible conformations—two chair and one boat—which are interchangeable by less than 0.5 Kcal/mole.

When the three conformers of Sorbinil, *3*, quercetin, *5*, 3-hydroxy-11-oxo-11*H*-pyrido[2,1*b*]quinazoline-8-carboxylic acid, *7*, and 1-phenyl-spiro-indole-1,2,3*H*-2-oxo-3,4′-imidazolidin-2′,5′-dione, *10*, of Table 1 are superimposed in a planar conformation upon each other at the A-ring (*shaded* in Table 3) of each molecule, the molecular conglomerate of Fig. 3 A and B is formed. This generally planar figure, which can essentially encompass the molecular structures of most known inhibitors, consists of two coplanar aromatic regions, a primary region formed by the superimposition of the A-rings (*shaded*) and a broad secondary region that is more widely dispersed. This is more clearly illustrated in the space-filling model of Fig. 4A and B, in which Fig. 4A corresponds to the back view (Fig. 3B).

TABLE 2

Net charge distribution of aldose reductase inhibitors when placed in a planar conformation

no.	Net charge distribution	no.	Net charge distribution
1	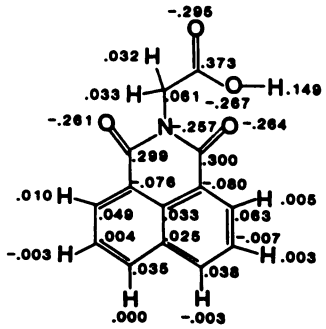	6	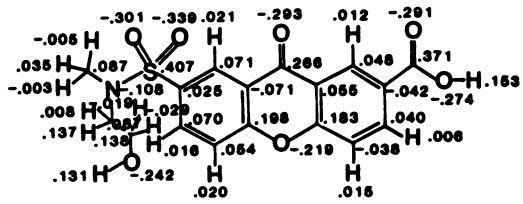
2	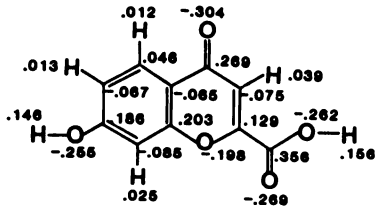	7	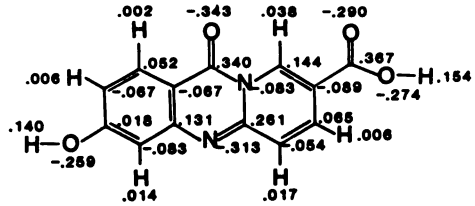
3	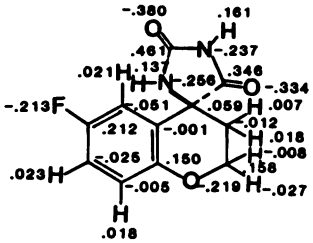	8	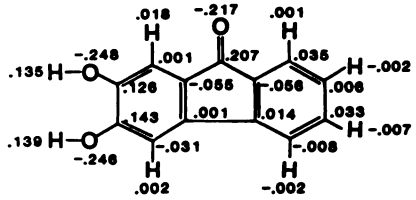
4	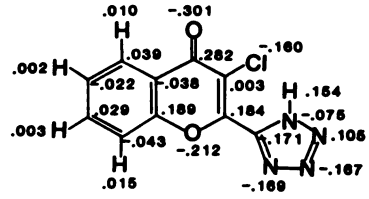	9	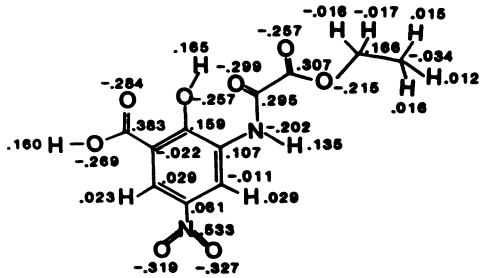
5	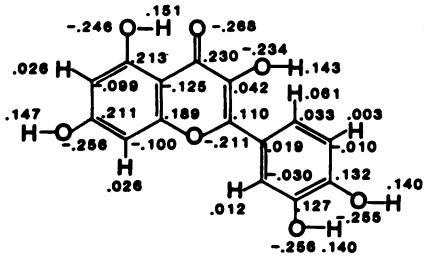	10	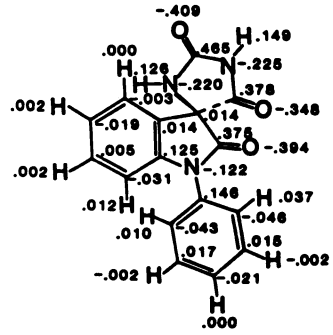

Aside from the overlap of the aromatic ring systems, a common feature of these inhibitors is the apparent broad overlap of carbonyl regions, which are susceptible to nucleophilic attack. As illustrated by distance measurements from the carbonyl (*shaded*) to the plane generated by the A-ring (*shaded*) in Table 3, these carbonyl groups vary from being essentially coplanar with the plane generated by the A-ring to being directed below the plane of the A-ring. Moreover, with the exception of the oxanilic ester *9*, all carbonyl groups are essentially sterically locked in the molecule as part of a rigid ring system. However, conformational changes in the rigid spirohydantoin *3* can slightly alter the spacial relationship between the carbonyl group and the plane generated by the

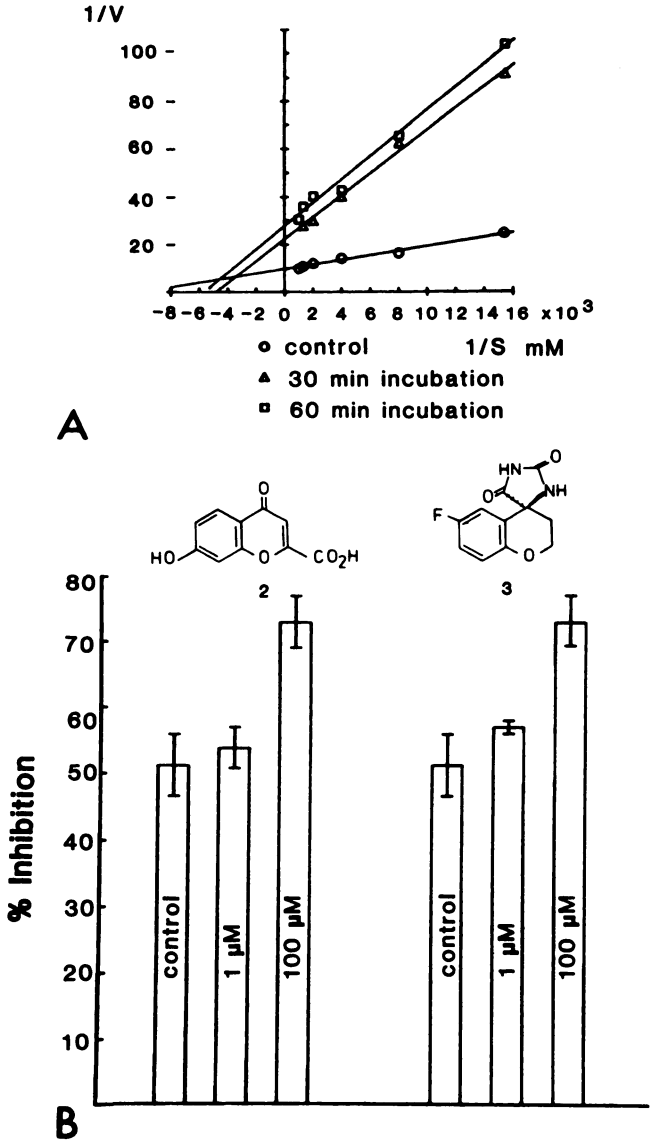

FIG. 2. *BrNAP incubation with HPAR*

A. Lineweaver-Burke plot of 1 mM BrNAP incubated with purified HPAR for 30 min (△) and 60 min (□). The substrate was DL-glyceraldehyde. Velocity units are changes in A_{340}/4 min.

B. Competition studies of 7-hydroxy-4-oxo-4*H*-chromen-2-carboxylic acid, *2*, and Sorbinil, *3*, at indicated concentrations with HPAR incubated overnight with 1 mM BrNAP (control).

All points in A and B represent the means of four to six determinations.

ring. Therefore, the values for Sorbinil, *3*, in Table 3 represent measurements for the more stable conformer, although distances varied from −1.14 to −1.38 Å for carbon and from −2.27 to −2.45 Å for oxygen. In Compound *9*, the carbonyl group is part of a freely rotating oxanilic acid residue. Rotation of the phenyl C—N carbonyl bond by 22.5° from a conformation in which the carbonyl group is coplanar with the aromatic ring results in a favorable carbonyl positioning with an expenditure of 3.4 Kcal/mole from the apparent lowest-energy conformation formed by a 20° twist.

Distance measurements, conducted from the center of the A-ring to the carbon and oxygen atoms of the carbonyl, also indicated spatial similarities. Values for all compounds ranged from 2.84 to 3.78 Å for the carbon and from 3.60 to 4.96 Å for the oxygen from the center of the *shaded* A-rings (Table 3). Overlap of the apparent common carbonyl regions, which are partially buried under position 4 of the spirobenzopyran in Fig. 4A and B, are indicated in *blue*.

Since inhibition is not competitive, the inhibition of aldose reductase can be postulated to result from several mechanisms. These include either an alteration of the 3-dimensional structure of the enzyme, produced upon binding of the inhibitor, which in turn leads to a distortion of the catalytic site, or to a steric interference of the catalytic site produced by partial overlapping of the bound inhibitor with the catalytic site. Either of these possibilities could be envisoned to result from simple nucleophilic attack of the reactive carbonyl by the tyrosine to form a reversible tetrahedral intermediate. Alternatively, the carbonyl group could act as a "charge-transfer" bridge between an "acidic" and "basic" group on the enzyme, thus allowing them to interact reversibly, the net result of such an interaction being a conformational change that results in inhibition. This latter possibility is illustrated in Fig. 4C and D by the introduction of tyrosine and arginine residues, arbitarily positioned in real-time on the Evans and Sutherland system to the inhibitor conglomerate. In this position (Table 3), the hydroxyl oxygen of tyrosine ("basic residue") can readily interact with the carbonyl carbon of each inhibitor, separated by 2.25–3.36 Å, whereas the imine hydrogen of arginine ("acidic residue") can interact with the carbonyl oxygen, separated by 1.56–3.65 Å.

Currently, no evidence exists for such an interaction between arginine and tyrosine and its inclusion here is used only to illustrate the possibility for such a reversible charge-transfer interaction between an "acidic" and "basic" residue on the aldose reductase enzyme. Doughty *et al.* (30), however, have reported the presence of both arginine and tyrosine at or near the nucleotide fold of BLAR. We have also confirmed the presence of arginine in the nucleotide cofactor fold through the use of the arginine-specific reagent camphorquinone-10-sulfonic acid.[2]

By combining the observations of Figs. 3 and 4 with known structure-activity relationships of aldose reductase inhibitors, one can postulate a site onto which this inhibitor model may fit. At this site, a three-point interaction with the inhibitors could be expected to occur. This includes hydrophobic interactions between a primary lipophilic region on the enzyme (1°) and the A-ring aromatic region of the inhibitor, hydrophobic interactions between a secondary lipophilic region (2°) and the broad secondary aromatic inhibitor region on some inhibitors, and a "charge-transfer" interaction with the nucleophilic carbonyl. This can be schematically visualized in the proposed model of Fig. 5, which consists of two planar lipophilic areas and a sterically constrained charge-transfer pocket that contains a nucleophilic amino acid. The two lipophilic regions, which also possess

[2] P. F. Kador and N. E. Sharpless, unpublished data.

TABLE 3

Measurement of various molecular distances

no.	Structure	Distance (Å) from plane generated by A ring* to carbonyl* C	O	Distance (Å) from center of A ring* to carbonyl* C	O	Distance (Å) from basic (B) and acidic (A) groups of model to carbonyl* B - C	A - O
1	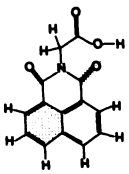	-.01	.01	3.78	4.96	3.36	3.65
2	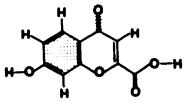	-.02	-.21	2.85	3.65	3.11	2.75
3	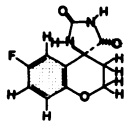	-1.38	-2.45	3.65	3.84	2.48	2.03
4	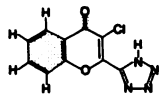	-.02	-.02	2.85	3.65	3.11	2.75
5	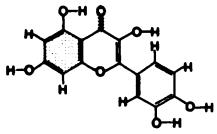	-.02	-.02	2.85	3.65	3.11	2.75
6	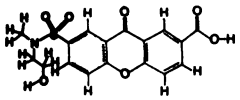	.00	.01	2.84	3.63	3.13	2.75
7	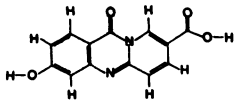	.07	.07	2.92	3.60	3.13	2.74
8	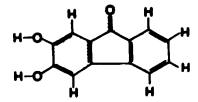	.00	.01	3.82	3.71	3.10	2.96
9	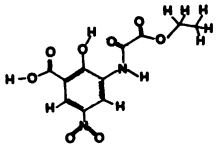	-1.01	-2.03	3.71	3.76	2.29	1.56
10	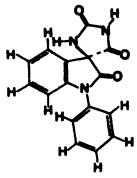	-1.15	-2.30	3.78	4.01	2.25	2.24

*Shaded

hydrogen-bonding sites near the positions indicated by *H*, are either coplanar (Fig. 5B) or parallel with the secondary lipophilic region formed in part by tyrosine, as suggested in Fig. 4C and D.

Assuming compounds with a higher affinity for a receptor are more potent agonists in vitro, one could postulate that enhancing the lipophilic properties of the aromatic regions of the inhibitor should result in higher

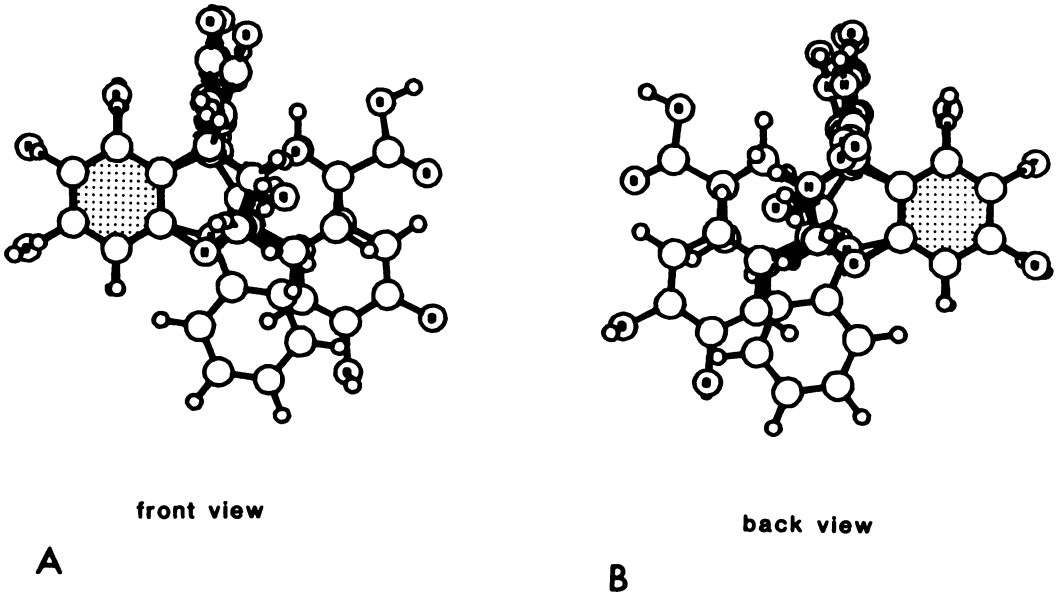

FIG. 3. *Molecular conglomerate formed upon superimposition of the A-rings (shaded) of the three conformers of Sorbinil, 3, quercetin, 5, 2-hydroxy-11-oxo-11H-pyrido[2,1b]quinazoline-8-carboxylic acid, 7, and 1-phenyl-spiro-indole-1,2,3H-2-oxo-3,4'-imidazolidin-2',5'-dione, 10, from Table 3 as viewed from the front (A) and rear (B).*

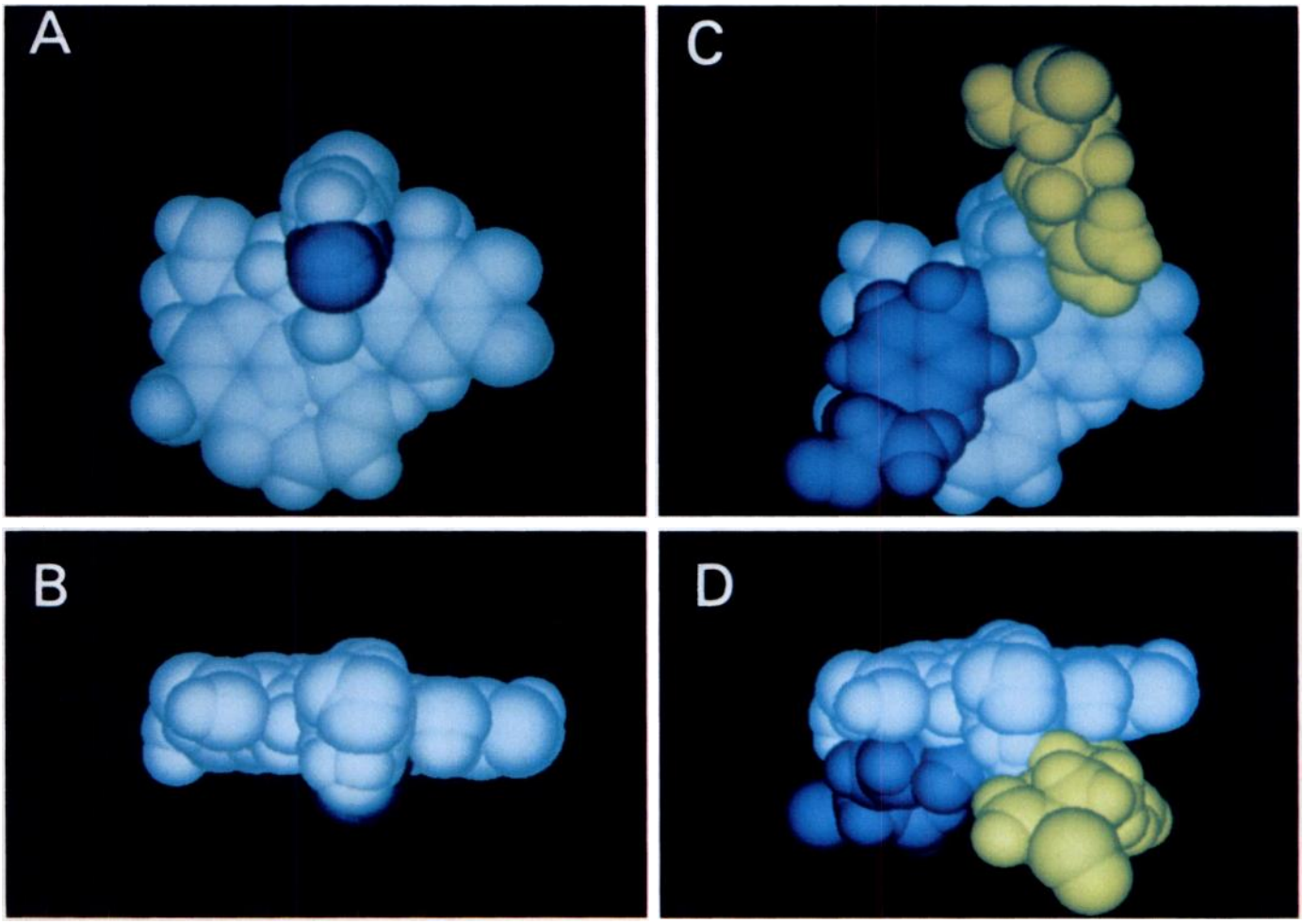

FIG. 4. *CPK molecular conglomerate formed upon superimposition of the A-rings*

Various inhibitors in Table 1 as viewed from the rear (A) and top (B). A corresponds to Fig. 3B. The superimposed A-rings are at the *right*, and the *dark blue* indicates areas of apparent overlap of the common carbonyl regions. C and D represent the rear (C) and top (D) views illustrating the ability of the common carbonyl regions to serve as a "charge-transfer" bridge between a tyrosine (*yellow*) hydroxyl group and an acidic imminium hydrogen of arginine (*blue*).

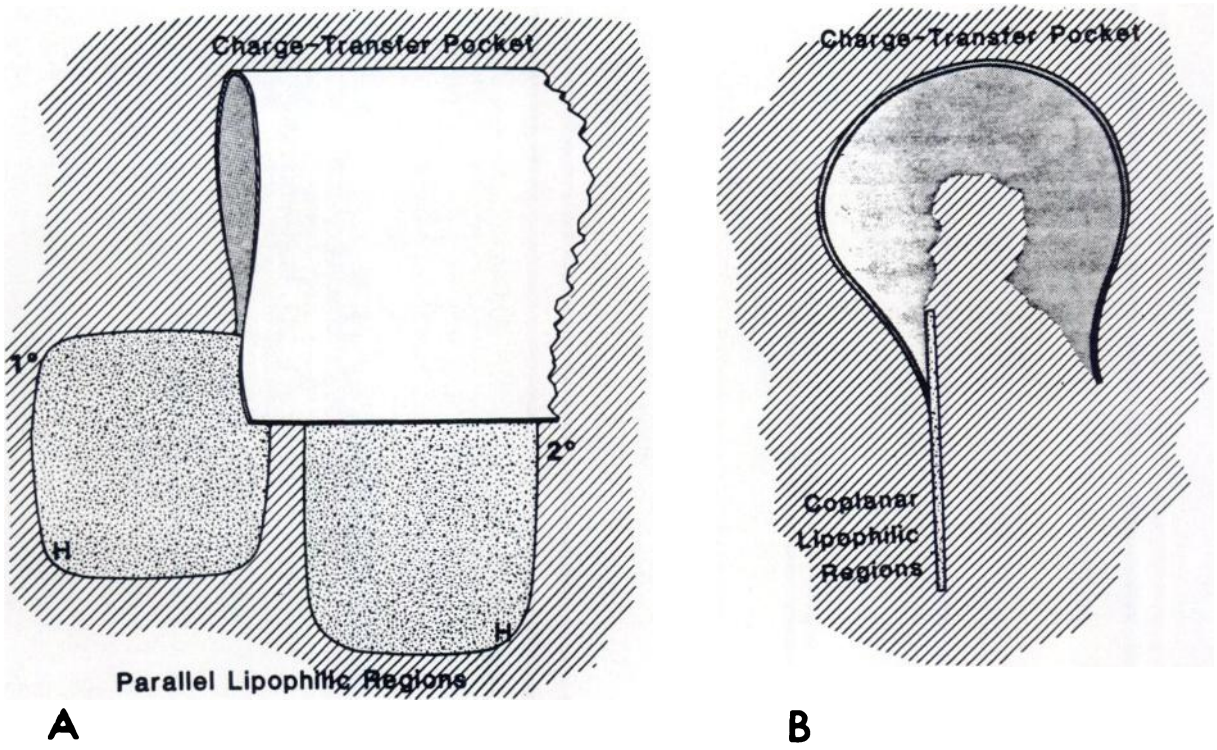

FIG. 5. *Front (A) and side (B) views of the postulated aldose reductase inhibitor site model*
This site consists of either two parallel or coplanar lipophilic regions [primary (1°) and secondary (2°)], each containing a hydrogen-bonding site (*H*) and a sterically constrained charge-transfer pocket. The 1° site (*left*) interacts with the region formed by the overlap of the inhibitor A-rings (*left* on Fig. 2A).

affinity for the inhibitor site and, subsequently, higher inhibitor potency. This can be seen in published observations which show that introduction of hydrophobic groups, which can increase the lipophilicity of the inhibitors, increases *in vitro* inhibitory activity (Table 4). First observed in the halogen substitution of Alrestatin, *2*, similar enhancement of activity has been reported with dichloro analogues of Sorbinil or related spiro-thiazolidine analogues (19, 20). Introduction of acetal moieties

TABLE 4
Evidence for hydrophobic interactions

Compound	no.	R_1	R_2	X	IC_{50} BLAR μM
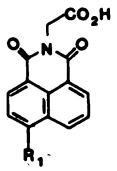	1	H			7.5
	11	Cl			1.3
	12	SC_6H_5			0.5
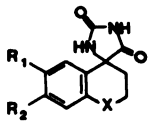	13	H	H	O	13
	3	F	H	O	3.4
	14	Cl	H	O	<0.1
	15	Cl	Cl	O	<<0.1
	16	H	H	S	7.4
	17	F	H	S	0.3
	18	Cl	H	S	0.4
	19	Cl	Cl	S	<0.1
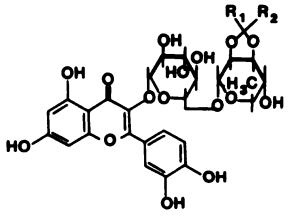	20	CH_3	CH_3		22
	21	CH_3	Et		8.1
	22	CH_3	Bu		5.3

TABLE 5
Evidence for a hydrogen-bonding effect

Compound	no.	R	IC_{50} RLAR μM
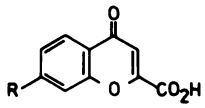	23	H	400
	2	OH	2.2
		OCH_3	29
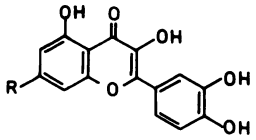	5	OH	0.8
	25	OCH_2CH_2OH	3.0
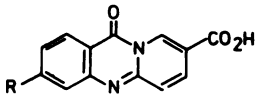	26	H	42
	7	OH	1.3
	27	OCH_3	140
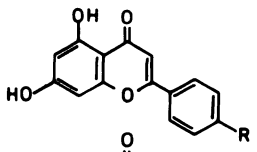	28	H	8.0
	29	OH	1.0
	30	OCH_3	5.0
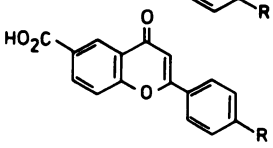	31	H	17% at 1×10^{-4}
	32	OH	3.2

to the 3-substituted sugar moieties of flavonoids has also been reported to increase the inhibitory activity by increasing the lipophilicity of these compounds (22).

In addition to hydrophobic interactions, hydrogen-bonding sites near each of the two lipophilic regions can also help to orient less lipophilic inhibitors containing hydroxyl substituents to the inhibitor site. As seen in Table 5, etherification of the 7-hydroxyl group of either the chromone carboxylic acid, *2*, and quercetin, *5*, or the 3-hydroxyl group of the pyrido[2,1*b*]quinazoline carboxylic acid, *7*, decreases the inhibitory activity of these compounds, presumably by decreasing their ability to hydrogen-bond to the bonding site at or near the primary lipophilic region. However, this hydrogen bonding interaction would not be expected to result in an all-or-none inhibition effect with these compounds since etherification of the hydroxyls can also increase the lipophilicity of the inhibitors. Evidence for a bonding site at or near the secondary lipophilic region is seen in the methylation of 2-(4′-hydroxy)-5,7-dihydroxy-4-oxo-4*H*-chromen, *11*, and more dramatically in the introduction of a 4′-hydroxy substituent to 2-phenyl-6-carboxy-4-oxo-4*H*-chromen, *31*.

A rational model for the aldose reductase inhibitor site must also predict the experimentally observed stereospecific recognition of inhibitors. From the location of the lipophilic binding regions and the "charge-transfer" pocket, potential stereochemical recognition of a chiral inhibitor is possible. This stereochemical recognition can be illustrated with the spiro-hydantoin Sorbinil, *2*, which fits the proposed inhibitor site as illustrated in Fig. 6. One can readily observe that the reactive carbonyl of only one enantiomer can properly participate in the charge transfer. Therefore, the 1-carbonyl of the hydantoin ring of the active *S*-enantiomer can serve as a charge transfer bridge whereas in the less active *R*-enantiomer the carbonyl is improperly positioned.

Proposed bulk tolerance differences between HLAR, HPAR, and RLAR have been postulated to account for differences in the susceptibility of these enzymes to inhibition. Although specific steric differences between these enzymes is still unknown, bulk tolerance differences have been partially incorporated into this proposed model through the introduction of a sterically constrained charge-transfer pocket. In HPAR, this charge transfer pocket is believed to be more sterically constrained than in either HLAR or RLAR. Therefore, inhibitors with subsituents which must extend into this pocket in order for the inhibitor to fit the inhibitor site properly would be expected to be less potent against HPAR. This is illustrated in Fig. 7 with 3′-carboxy-2′-hydroxy-5′-nitro-oxanilic acid, ethyl ester, *9*, which is 73-fold less potent in HPAR than in RLAR. The oxanilic ester portion of this compound extends into the sterically restricted charge-transfer pocket in order for this molecule to fit the inhibitor site properly (Fig. 7).

In general, the search for aldose reductase inhibitors has employed random screening techniques. With an understanding of the molecular mechanism of action and the pharmacophor requirements of these inhibitors, more potent and specific inhibitors can be rationally designed. Having combined the results obtained from molecular modeling of the inhibitors with observations of the proposed inhibitor site, we propose the following pharmacophor requirements, summarized in Fig. 8. The minimal requirements consist of a primary aromatic region and a

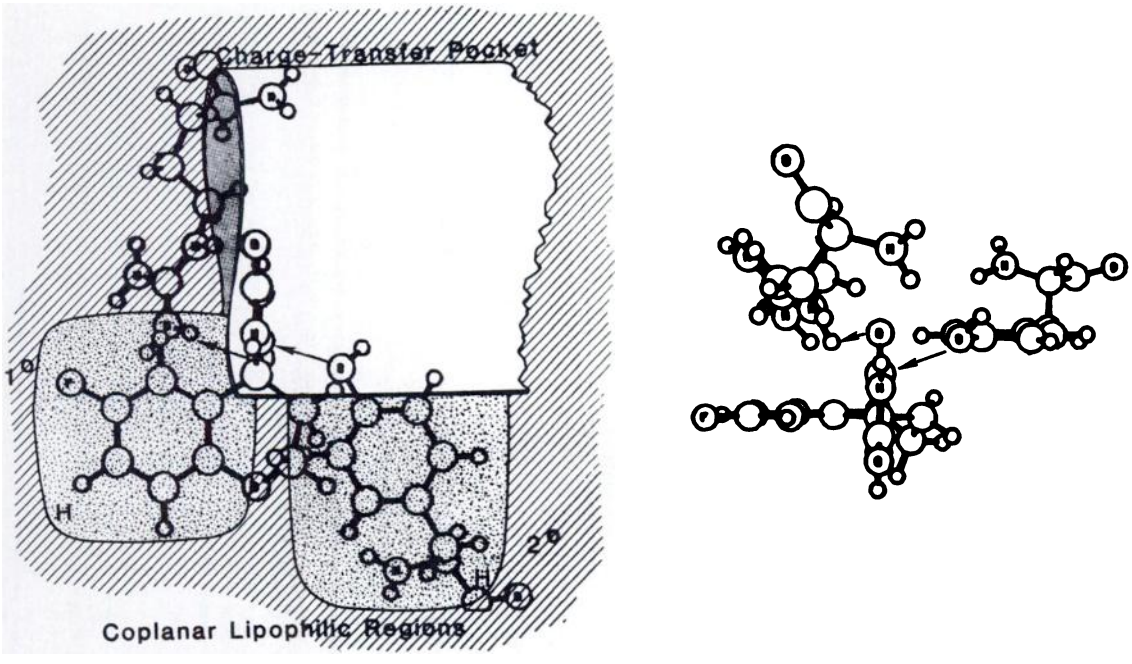

FIG. 6. *Front (A) and top (B) views illustrating the stereospecific recognition of the inhibitor Sorbinil, 3*

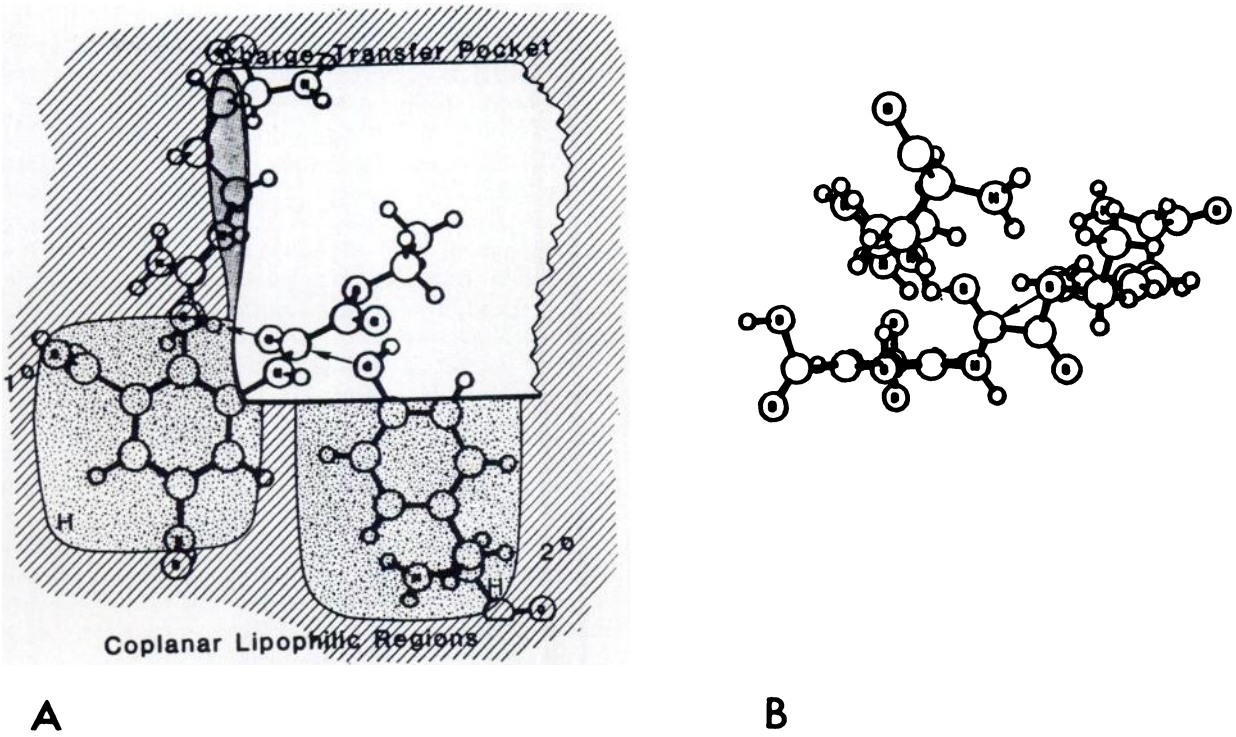

FIG. 7. *Steric restrictions in the charge-transfer pocket [front (a), top (b)] illustrated by 3'-carboxy-2'-hydroxy-5'-nitro-oxanilic acid, ethyl ester, 9, whose oxanilic acid portion extends into the pocket in order for this molecule to properly fit the inhibitor site*
This compound is 73-fold less active against HPAR than against RLAR.

carbonyl group separated by 2.8–3.8 Å (d_1, defined as the distance between the center of the aromatic ring to the carbon of the carbonyl). Hydrophobic bonding is enhanced upon introduction of a secondary planar aromatic and/or lipophilic region centered around 2.8–6.1 Å from the carbonyl. Two hydroxyl groups located 2.8–3.8 Å and 8.0–9.3 Å from the center of the primary aromatic ring also help to bind the inhibitor to the inhibitor site.

ACKNOWLEDGMENT

We wish to thank Mr. Richard Feldmann, of the National Institutes of Health Division of Computer Research and Technology, for his help on the Evans and Sutherland system.

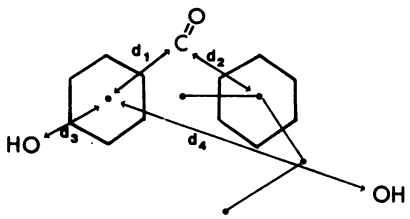

Approximate Distances

d_1	2.8–3.8 Å
d_2	2.8–6.1 Å
d_3	2.8–3.8 Å
d_4	8.0–9.3 Å

FIG. 8. *Pharmacophor requirements of the aldose reductase inhibitors*
Distances are measured from the center of the aromatic ring of the specific atoms.

REFERENCES

1. Kinoshita, J. H., S. Fukushi, P. Kador, and L. O. Merola. Aldose reductase and complications of the eye. *Metabolism* **28**:462–469 (1979).
2. Corder, C. N., J. M. Braughler, and P. A. Culp. Quantitative histochemistry of the sorbitol pathway in glomeruli and small arteries of human diabetic kidney. *Folia Histochem. Cytochem.* **17**:137–146 (1979).
3. Bidot-Lopez, P., S. Robertson, and B. C. O'Mallay. Sorbitol accumulation in human diabetic and in normal platelets incubated in glucose. *Clin. Res.* **27**:363A (1979).
4. Fukushi, S., L. O. Merola, and J. H. Kinoshita. Altering the course of cataracts in diabetic rats. *Invest. Ophthalmol. Visual Sci.* **19**:313–318 (1980).
5. Datiles, M. B., P. F. Kador, H. N. Fukui, T.-S. Hu, and J. H. Kinoshita. Corneal re-epithelialization in galactosemic rats. *Invest. Ophthalmol. Visual Sci.* **24**:563–569 (1983).
6. Judzewitsch, R., J. B. Jaspan, K. S. Polonsky, C. R. Weinberg, J. B. Halter, E. Halar, M. A. Pfeifer, C. Vukadinovic, L. Bernstein, M. Schneider, K.-Y. Liang, K. H. Gabbay, A. H. Rubsenstein and D. Porte, Jr. Aldose reductase inhibition improves motor nerve conduction velocity in diabetic patients. *N. Engl. J. Med.* **308**:119–125 (1983).
7. Kador, P. F., and N. E. Sharpless. Structure-activity studies of aldose reductase inhibitors containing the 4-oxo-4H-chromen ring system. *Biophys. Chem.* **8**:81–85 (1978).
8. P. F., Kador, J. D. Goosey, N. E. Sharpless, J. Kolish, and D. D. Miller. Stereospecific inhibition of aldose reductase. *Eur. J. Med. Chem.* **16**:293–298 (1981).
9. Kador, P. F., J. H. Kinoshita, W. H. Tung, and L. T. Chýlack. Differences in the susceptibility of aldose reductase to inhibiton. II. *Invest. Ophthalmol. Visual Sci.* **19**:980–982 (1980).
10. Kador, P. F., L. O. Merola, and J. H. Kinoshita. Differences in the susceptibility of aldose reductase to inhibition. I. *Doc. Ophthalmol. Proc. Ser.* **18**:117–124 (1979).
11. Kador, P. F., D. Carper, and J. H. Kinoshita. Rapid purification of human pacental aldose reductase. *Anal. Biochem.* **114**:53–58 (1981).
12. Rindone, W. P., and T. Kush. *PROPHET Molecules: a User's Guide to the Molecular Facilities of the PROPHET System.* Bolt Beranek and Newman, Inc., Cambridge, Mass. (1980).
13. Cameron, A., and N. Cameron. The stereochemical basis of anticonvulsant drug action: the crystal and molecular structure of diphenylhydantoin, a noncentrosymmetric structure solved by centric symbolic addition. *Acta Crystallogr. Sect. B.* **27**:2205–2211 (1971).
14. Cohen, N. C. GEMO, a computer program for the calculation of the preferred conformations of organic molecules. *Tetrahedron* **77**:789–797 (1971).
15. Pople, J. A., and D. L. Beveridge. *Approximate Molecular Orbital Theory.* McGraw-Hill, New York (1970).

16. Feldmann, R. J. The design of computing systems for molecular modeling. Annu. Rev. Biophys. Bioeng. 5:477–509 (1976).
17. Horner, L., and D. W. Baston. Versuche zur Darstellung von Chinonen des Fluorens und des Fluorenons. *Liebigs Ann. Chem.* 910–935 (1973).
18. Doria, G., C. Romeo, P. Giraldi, F. Lauria, P. Sberze, M. Tibolla, M. L. Corno, G. Cadelli, and C. Montoro. Antiallergy agents. I. Substituted 4-oxo-4*H*-1-benzopyran-6-carboxylic acids. *Eur. J. Med. Chem.* 13:33–39 (1978).
19. Sestanj, K. 1*H*-Benz[de]isoquinoline-2(3*H*)-acetic acid derivatives. United States Patent 4,254,109 (1981).
20. Sarges, R. Spiro-hydantoin Verbindungen und ihre Verwendung. German Patent 27 46 244 (1977).
21. Fauran, F., C. Fenion, J. Mosser, and G. Prat. Acetals derives de glycosides de la Quercetine inhibiteurs de l'aldose reductase. *Eur. J. Med. Chem.* 13:503–508 (1978).
22. Varma, S. D., and J. H. Kinoshita. Inhibition of lens aldose reductase by flavonoids. *Biochem. Pharmacol.* 25:2505–2513 (1976).
23. Pfister, J. R., and L. D. Waterbury. Synthesis and aldose reductase inhibitory activity of 7-sulfamoylxanthone-2-carboxylic acids. *J. Med. Chem.* 23:1264–1267 (1980).
24. Brittain, D. R. 1′-Substituted-spiro(1-imidazolidine-4,3′-indoline-2,2′,5)-triones, process for their manufacture and pharmaceutical composition thereof. European Patent Application 0 028 906 (1980).
25. Inagaki, K., M. Ichimoto, T. Yashiro, and J. Okuda. Inhibition of aldose reductases from rat and bovine lenses by hydantoin derivatives. *Chem. Pharm. Bull.* 30:3244–3254 (1982).
26. Kador, P. F., N. E. Sharpless, and J. D. Goosey. Aldose reductase inhibition by anti-allergy drugs, in *Enzymology of Carbonyl Metabolism: Aldehyde Dehydrogenase and Aldo/Keto Reductase.* (H. Weiner and B. Wermuth, eds.). Alan R. Liss, New York, 243–260 (1982).
27. Cheney, B. V., J. B. Wright, C. M. Hall, H. G. Johnson, and R. E. Christoffersen. Structure-activity correlations for a series of antiallergy agents, oxanilic, quinaldic and benzopyran-2-carboxylic acids. *J. Med. Chem.* 21:936–940 (1978).
28. Ferrell, J. E., Jr., P. D. G. Chang Sing, G. Loew, R. King, J. M. Mansour, and T. E. Mansour. Structure/activity studies of flavonoids as inhibitors of cyclic AMP phosphodiesterase and relationship to quantum chemical indices. *Mol. Pharmacol.* 16:556–568 (1979).
29. Liao, T. H. Modification of bovine pancreatic DNase with *p*-nitrobenzenesulfonyl fluoride at tyrosine residues. *Fed. Proc.* 40:1613 (1981).
30. Doughty, C. C., S.-M. Lee, S. Conrad, and S. Schade. Kinetic mechanism and structural properties of lens aldose reductase, in *Enzymology of Carbonyl Metabolism: Aldehyde Reductases and Aldo/Keto Reductase* (H. Weiner and B. Wermuth, eds.). Alan R. Liss, New York, 223–242 (1982).

Send reprint requests to: Dr. Peter F. Kador, Building 6, Room 237, National Eye Institute, Bethesda, Md. 20205.